

TRANSIENT ANALYSIS OF BODIES WITH MOVING BOUNDARIES USING NASTRAN

John W. Frye

Naval Underwater Systems Center

SUMMARY

A scheme is presented which allows the modeling of a moving boundary with NASTRAN NOLIN cards. Various aspects and limitations of the approach are explained. Recommendations are given as to the procedure to be used in implementing the method.

INTRODUCTION

Situations occasionally arise when the boundary conditions of a theoretical model change as a result of the response of the model. The case under consideration is that where the boundaries of the model move as a function of rigid body displacement. The problem which motivated the development of the technique which is presented here is that of a shaft under both axial and transverse loading moving between two stationary bearings. Figure 1 is a diagram of such a shaft.

The reactions at the bearings are dependent on the applied loadings and the inertial forces generated by transverse motions of the shaft. The applied loadings are known beforehand. The inertial loadings of the shaft are unknown since the transverse motion of the shaft is an unknown. Therefore, the reactions of the bearings cannot be predetermined before the start of the analysis.

Constraints cannot be directly applied to the model to account for the bearings since such constraints would be useful for only a short time of the analysis covering a small axial displacement of the shaft. It is possible to solve the problem by dividing the total time of the analysis up into many small time increments each with a different constraint condition. The idea here would be to start the analysis with the bearings in one position; run the problem for a short time; stop the analysis; change the constraints; and restart the problem with initial conditions equal to the state of the model at the end of the first time increment. This process is repeated until the shaft has moved as far as desired. This technique, while being possible, is awkward from the standpoint of data handling, the number of runs required, and the total number of days needed to obtain an answer.

SYMBOLS

distance between grid points

F_2 nonlinear loads at grid point accounting for moving boundary

$F_x(t), F_y(t)$	applied time dependent axial and transverse loads
i	index number of grid point
K	maximum slope of nonlinear loading curve
K_B	stiffness of bearing
s	scale factor
u_x, u_y	grid point axial and transverse displacements
x, y	axial and transverse coordinates of model
ξ	integration variable in axial direction

DISCUSSION

The approach which accounts for the moving bearings treated the bearings as stiff springs which moved along the model of the shaft as the shaft moved with respect to the bearings. These springs were fabricated artificially by the use of the nonlinear load option in NASTRAN. Each grid point along the shaft model over which the bearings could pass had two nonlinear loadings applied to it for each bearing. Figure 2 shows a diagram of these loadings for a typical grid point on the shaft model. For simplicity we consider the case of only one bearing.

The force F_2 is shown as a positive ramp function with a slope equal to the bearing stiffness and is a function of the displacement u_x of the shaft. The second force F_1 is shown as a negative ramp function with a slope equal to the bearing stiffness and is a function of the shaft displacement u_x added to the transverse deflection of the grid point u_y . Note here that since u_y is several orders of magnitude smaller than u_x , the magnitude of $u_x + u_y$ is mainly determined by u_x alone. Both F_1 and F_2 are zero until u_x is greater than x_{i-1} , the distance from the bearing at the start of motion to grid point $i-1$. F_1 and F_2 are equal and opposite and, hence, negate each other when u_x is greater than x_{i+1} , the distance from the bearing at the start of the motion grid point $i+1$. Therefore the loadings F_1 and F_2 add to zero at all times except those times when the bearing is between grid points $i-1$ and $i+1$.

Now consider a case when the bearing is between grid points $i-1$ and $i+1$. Figure 3 illustrates such a condition.

$$\text{NET LOAD} = F_1 + F_2 = -K(u_x + u_y - x_{i-1}) + K(u_x - x_{i-1})$$

$$\text{NET LOAD} = -Ku_y$$

As can be seen, the net load on the grid point i is equal to $-Ku_y$ which is a restoring force proportional to the bearing spring constant and the lateral deflection of the shaft at i . Thus, the combination of two nonlinear loadings at i results in simulating a bearing spring which turns itself on when the bearing is in the vicinity of grid point i and turns itself off when the bearing is outside the vicinity of grid point i .

It is possible to allow the spring constant of the bearing to vary as a function of its distance from a grid point. There is some advantage to this since when a bearing is between two grid points, its stiffness ought to be shared in some way by the two grid points. See figure 4.

We have used the proportional sharing scheme where the stiffness of the bearing is distributed in proportion to that of a load shared between two ends of a pinned ended beam. To establish the loading curve for this kind of stiffness sharing scheme, notice that

$$(1) \quad dF = Kd\xi = \left(K_B\right) \frac{\xi}{a} d\xi \quad 0 < \xi < a$$

$$(2) \quad dF = Kd\xi = \frac{K_B(2a - \xi)}{a} d\xi \quad a < \xi < 2a$$

From (1) noting $F = 0$ at $\xi = 0$

$$(3) \quad F = \int_0^x \left(K_B\right) \frac{\xi}{a} d\xi = \frac{K_B \xi^2}{2a} \Big|_0^x = \frac{K_B x^2}{2a} \quad 0 < x < a$$

$$\frac{\partial F}{\partial x} = \frac{K_B x}{a} \quad \frac{\partial F}{\partial x} = 0 \quad \text{at } x = 0$$

$$\frac{\partial F}{\partial x} = K_B \quad \text{at } x = a$$

$$F = \frac{K_B a}{2} \quad \text{at } x = a$$

From (2) noting $F = \frac{K_B a}{2}$ at $x = a$

$$F = \int_a^x \frac{K_B(2a - \xi)}{a} d\xi + \frac{K_B a}{2}$$

$$F = \frac{-K_B(2a - \xi)^2}{2a} \Big|_a^x + \frac{K_B a}{2} = K_B a - \frac{K_B(2a - x)^2}{2a}$$

$$(4) \quad F = K_B \left[a - \frac{(2a - x)^2}{2a} \right] \quad a < x < 2a$$

$$\frac{\partial F}{\partial x} = \frac{K_B(2a - x)}{a} \quad \frac{\partial F}{\partial x} = K_B \quad \text{at } x = a$$

$$\frac{\partial F}{\partial x} = 0 \quad \text{at } x = 2a$$

$$F = \frac{K_B a}{2} \quad \text{at } x = a$$

Equations (3) and (4) establish the shape of the loading functions for the proportional stiffness loading scheme. Other stiffness sharing schemes could be devised and their loading curves easily arrived at in a similar manner to that shown here. Figure 4 shows a plot of the nonlinear load function for the proportional stiffness sharing scheme we used.

The scheme depends completely on accurately determining the difference between the quantities $K(u_x + u_y)$ and Ku_x . Theoretically, this presents no difficulty. If the value of u_x is six or seven orders of magnitude larger than u_y , a numerical difficulty arises since a computer may only work to eight significant figures using single precision arithmetic. Even if double precision arithmetic is used, there will come a point where large values of u_x start to degrade the numerical accuracy of the differencing operation $K(u_x + u_y) - Ku_x$.

There is a way around this numerical difficulty. The objective of the differencing operation is to obtain the quantity Ku_y . If the u_x quantity is multiplied by a scalar constant the differencing operation remains unchanged.

$$K(su_x + u_y) - Ksu_x = Ku_y$$

Here u_x was multiplied by the scalar s . To remove the numerical difficulty, the scalar constant is assigned such that u_x is no more than three or four orders of magnitude greater than values of u_y which can possibly be of interest. su_x cannot be too small or else the larger values of u_y will start to affect the first few significant figures of the quantity $su_x + u_y$. This would result in inaccuracies in the determination of the spring constant since the spring constant should be a function of u_x only and not $su_x + u_y$. Thus, some judgment must be used in the determination of s ; that is to say it cannot be made some very small number without considering the values which u_y are expected to be in the neighborhood of a bearing.

When using the scalar multiplier the nonlinear loading diagram changes such that the nonlinear loads start to act at sx_{i-1} rather than at s_{i-1} , since the lock up function or independent variable is su_x rather than u_x . Figure 5 shows the forcing function set up using the scalar multiplier.

The equation for the nonlinear load as a function of su_x or $su_x + u_y$ now becomes

$$\frac{dF}{ds\xi} = K = K_B \frac{s\xi}{sa} \quad 0 < \xi < a$$

$$dF = sK \frac{\xi}{a} d\xi$$

$$F = \frac{sK_B x^2}{2a} \quad 0 < x < a$$

$$F = sK_B \left[a - \frac{(2a - x)^2}{2a} \right] \quad a < x < 2a$$

Differentiating with respect to sx yields

$$\frac{dF}{dsx} = \frac{d}{dsx} \left(\frac{K_B (s^2 x^2)}{2sa} \right) = \frac{2K_B sx}{2sa} = \frac{K_B x}{a} \quad 0 < x < a$$

$$\begin{aligned} \frac{dF}{dsx} &= \frac{dK_B}{dsx} \left[sa - \frac{(2as - sx)^2}{2sa} \right] \\ &= K_B \left[2 \frac{(2as - sx)}{2sa} \right] = K_B \frac{(2a - x)}{a} \quad a < x < 2a \end{aligned}$$

The slope of the nonlinear force curve with respect to the scaled coordinate remains the same as the slope of the force curve using an unscaled coordinate.

Figure 6 shows a typical result for the transverse displacement of a grid point in the analysis of a shaft moving between two bearings. The results show the expected suppression of transverse displacement while the bearings are in the vicinity of the grid point.

The application of nonlinear loads raises questions as to the numerical stability of the solution. The numerical stability will depend on the time step used and the maximum slope of the nonlinear force curves. If the moving boundary is a rigid one, some compromise must be made on the stiffness of the moving boundary. An infinite stiffness will always result in an unstable condition. In our case, we ran several short problems with our model using what we considered as a reasonable time step. We reduced the slope of the nonlinear load curves

until we obtained a stable solution and then reduced the time step until the solution appeared reasonably converged. This trial and error approach may not always work out, but it did in our case. We were able to arrive at an acceptable time step and loading slope within a few days. It is best when setting up the tables for the loading curves to set the maximum slope in the table to unity and to use the NOLIN cards to scale the slope. Thus, the maximum slope values will appear directly on the NOLIN cards. The tables are tedious to construct as there is a table for each grid point on the model over which the moving boundary must pass, whereas it is relatively easy to change the slope values on the NOLIN cards.

If the time steps are large, the slope of the nonlinear load curve must be very small in order to give good convergence and numerical stability. In such a case, the moving boundary cannot be accurately modeled using this method. This is unfortunate but as far as we can see, there is no alternative for solving the problems of convergence and stability other than to reduce the time step or the loading slope.

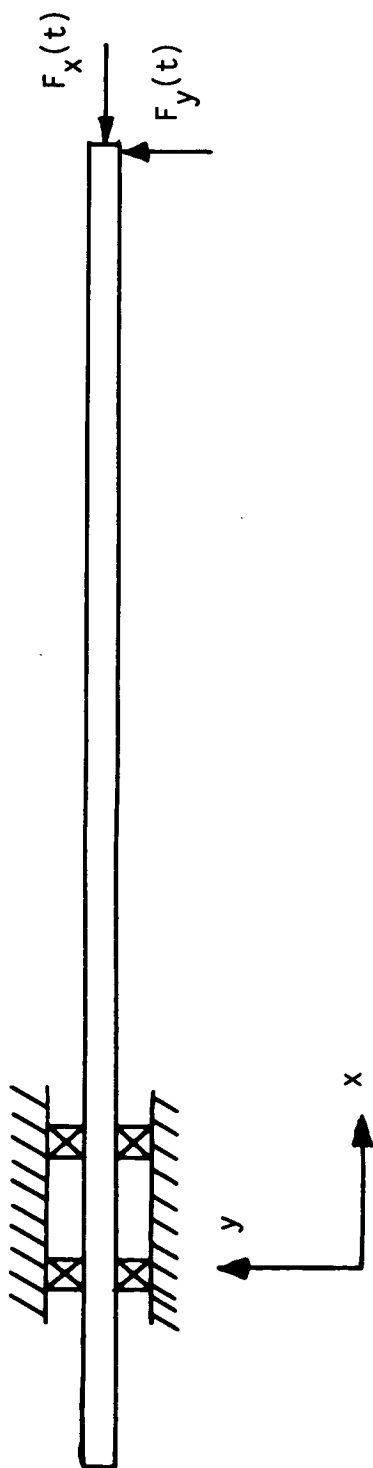


FIGURE 1. - SHAFT UNDER COMBINED TRANSVERSE AND RADIAL
LOADING FREE TO SLIDE BETWEEN TWO BEARINGS

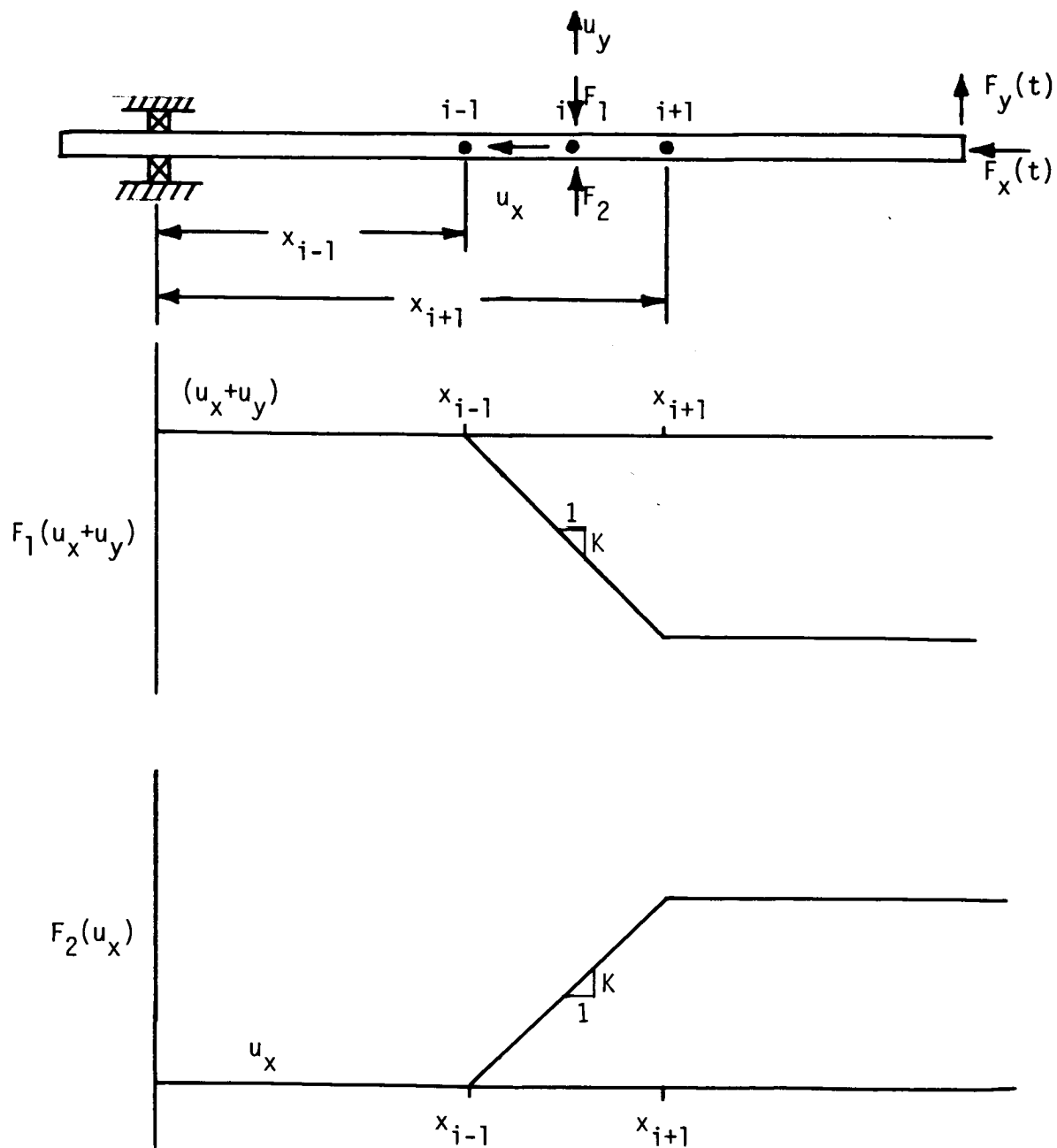
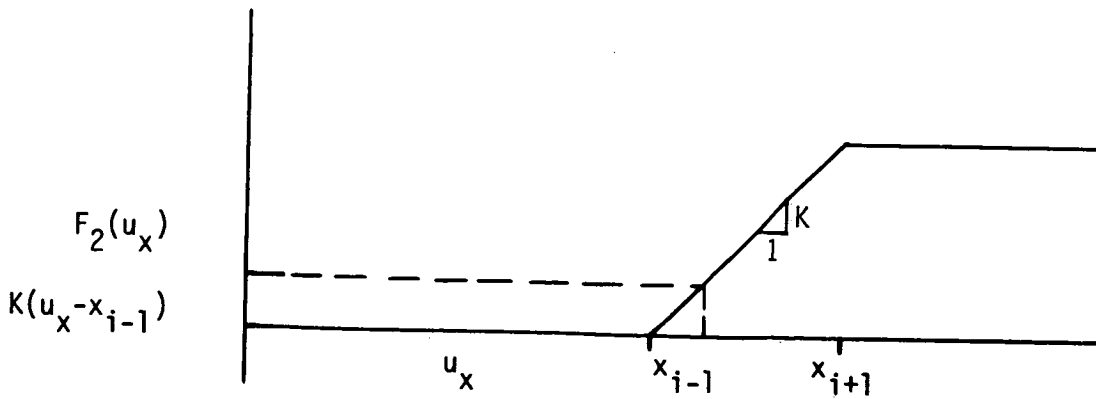
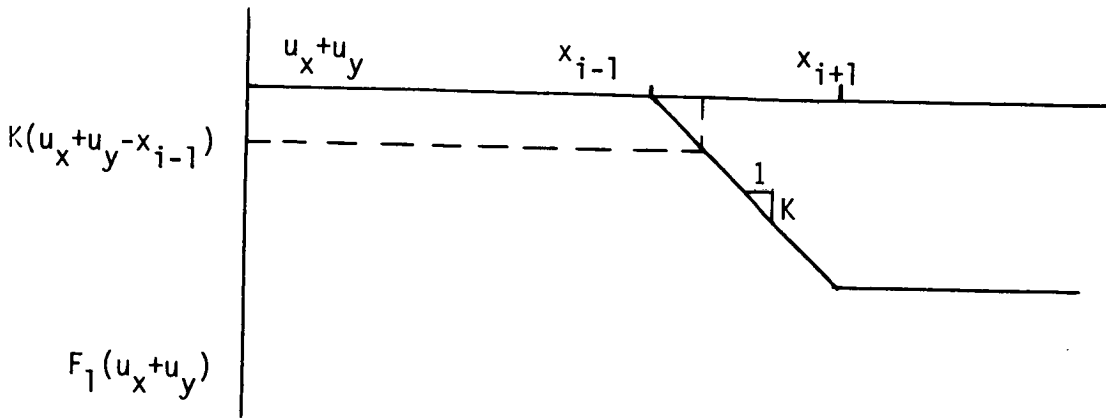
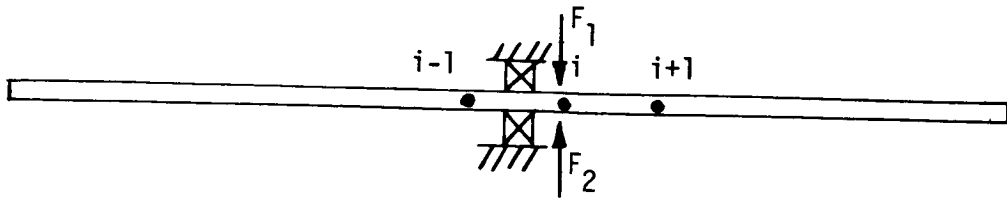
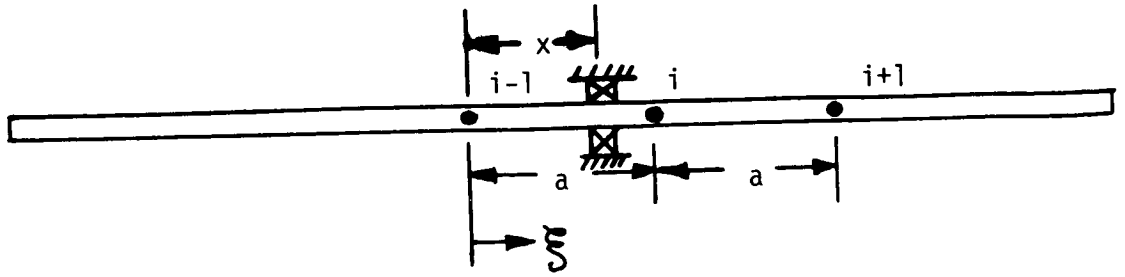


FIGURE 2. - NONLINEAR LOADING DIAGRAMS



$$\text{Net Load} = F_1 + F_2 = -Ks(u_x + u_y - x_{i-1}) + Ks(u_x - x_{i-1}) = -Ksu_y$$

FIGURE 3. - NONLINEAR LOADS WITH BEARING NEAR GRID POINT



$$K_{i-1} = K \frac{(a-x)}{a} \quad ; \quad K_i = K \frac{x}{a} \quad 0 < x < a$$

$$K_i = K \frac{(2a-x)}{a} \quad ; \quad K_{i+1} = K \frac{(x-a)}{a} \quad a < x < 2a$$

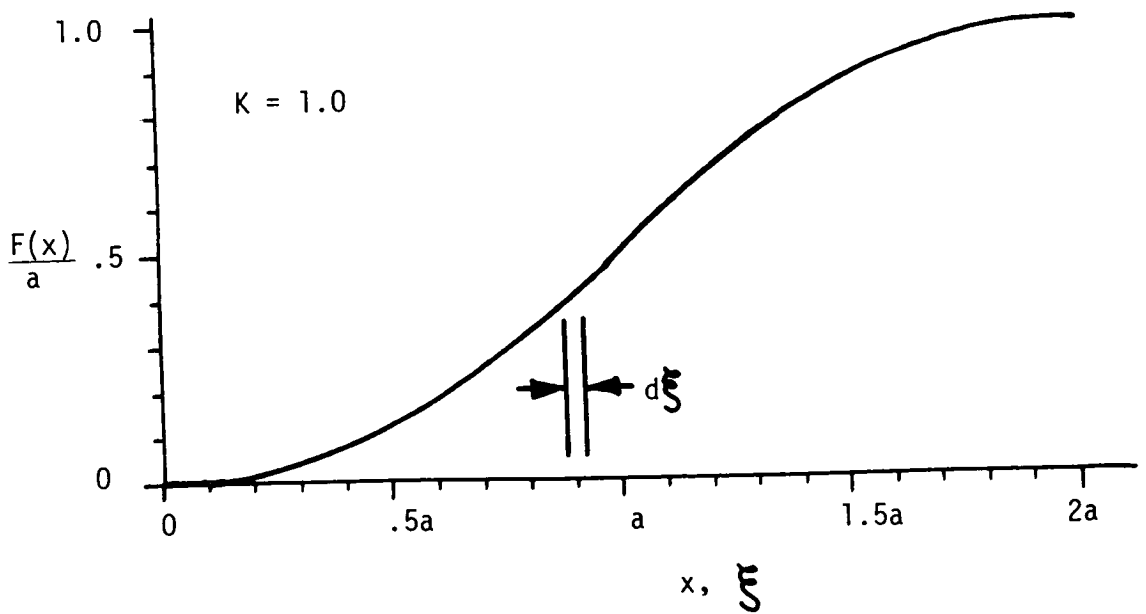


FIGURE 4. - PROPORTIONAL STIFFNESS SHARING SCHEME

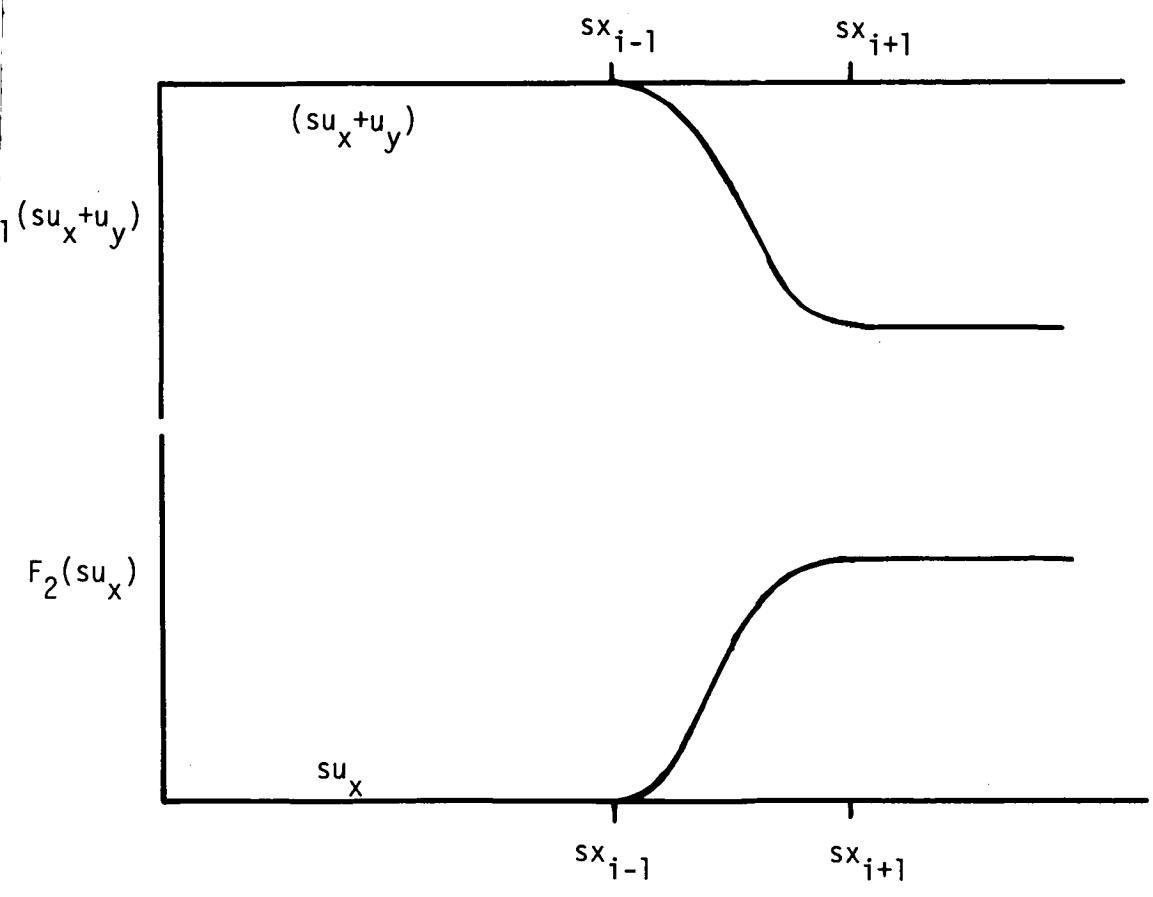
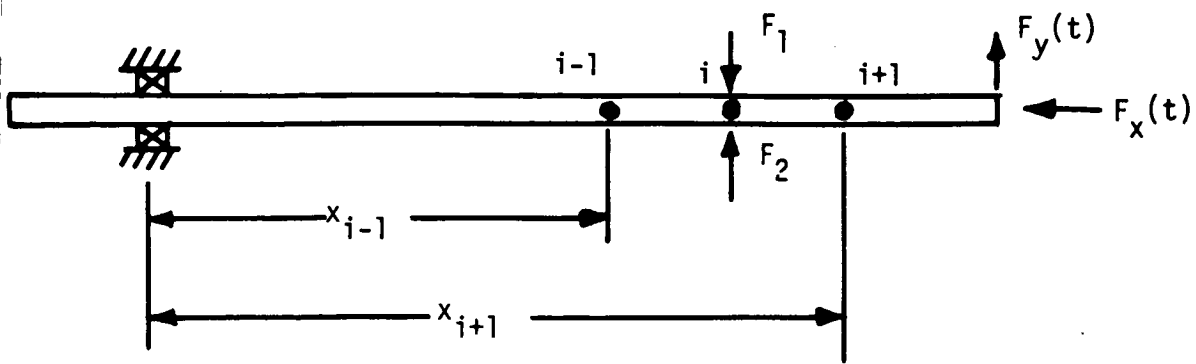


FIGURE 5. - ADDITION OF SCALE FACTOR s TO ELIMINATE ROUND OFF ERROR

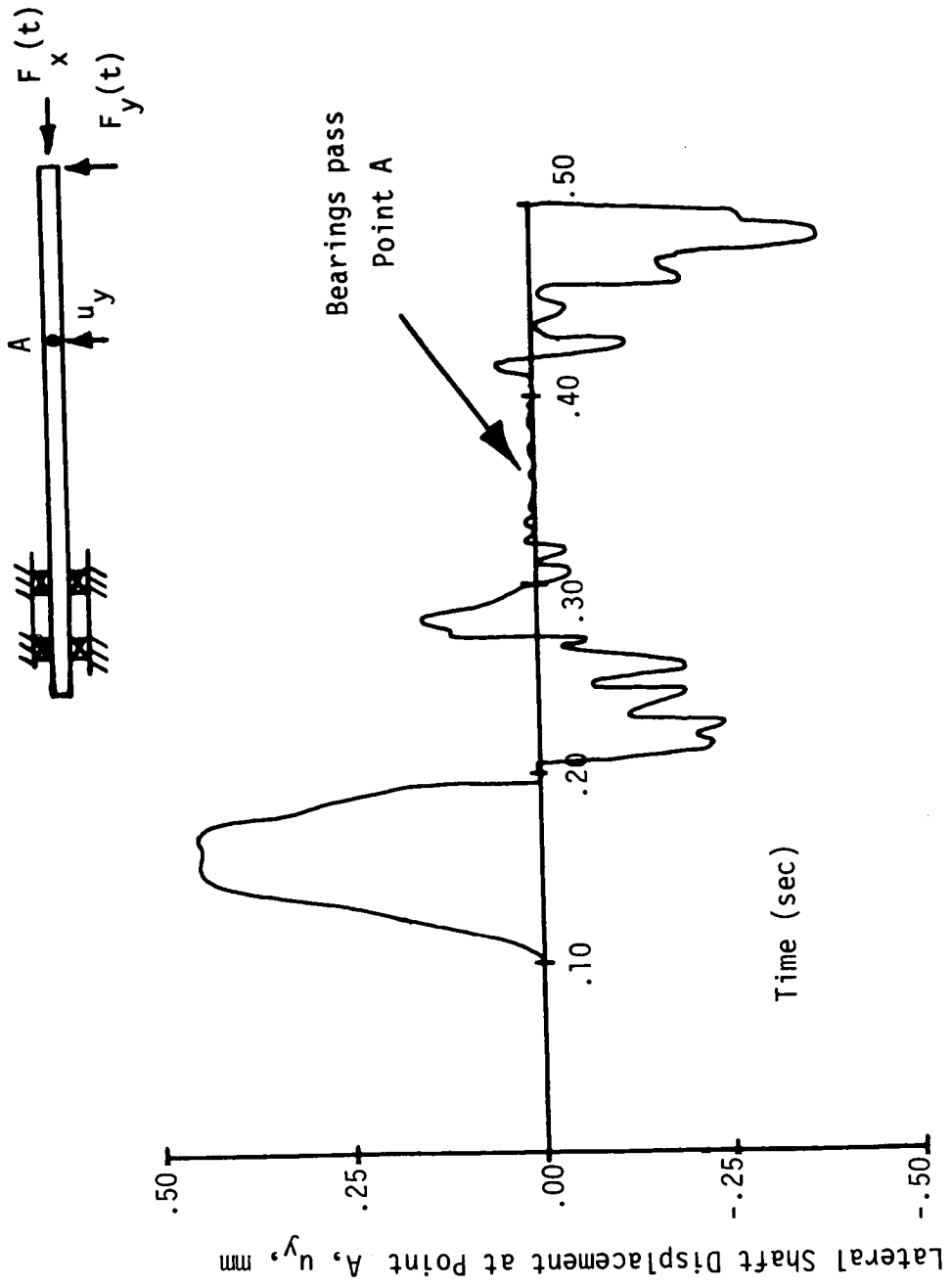


FIGURE 6. - TYPICAL RESULTS FOR LATERAL DISPLACEMENTS OF POINT ON SHAFT SLIDING BETWEEN TWO BEARINGS